Pulse Morphology Visualization and Analysis With Applications in Cardiovascular Pressure Signals

Tim Ellis*, *Student Member, IEEE*, James McNames, *Senior Member, IEEE*, and Mateo Aboy, *Member, IEEE*

***Abstract*—We present a new analysis and visualization method for studying the functional relationship between the pulse morphology of pressure signals and time or signal metrics such as heart rate, pulse pressure, and means of pressure signals, such as arterial blood pressure and central venous pressure. The pulse morphology is known to contain potentially useful clinical information, but it is difficult to study in the time domain without the aid of a tool such as the method we present here. The primary components of the method are established signal processing techniques, nonparametric regression, and an automatic beat detection algorithm. Some of the insights that can be gained from this are demonstrated through the analysis of intracranial pressure signals acquired from patients with traumatic brain injuries. The analysis indicates the point of transition from low-pressure morphology consisting of three distinct peaks to a high-pressure morphology consisting of a single peak. In addition, we demonstrate how the analysis can reveal distinctions in the relationship between morphology and several signal metrics for different patients.**

***Index Terms*—Arterial blood pressure (ABP), hemodynamics, intracranial pressure (ICP), point process, pulse contour analysis, pulse morphology, pulse pressure, traumatic brain injury (TBI).**

I. Introduction

CARDIOVASCULAR pressure signals such as arterial blood pressure (ABP), intracranial pressure (ICP), central venous pressure (CVP), and pulmonary arterial pressure (PAP) are frequently monitored and analyzed in both clinical and research environments. The mean pressure is the most well understood and clinically used metric for these signals. The mean pressure is technically defined as the average pressure over the duration of one cardiac cycle, though in practice it is often calculated as either a linear combination of the systolic and diastolic pressures or a 3–8 s moving window average.

Pressure signals contain much more information than is captured by the mean, systolic, and diastolic values. Most of this information can be extracted from the pulse morphology, which refers to the shape of a pressure signal over the span of a single cardiac cycle. In short signal segments, the pulse morphology is usually consistent, but it is known to change slowly over time. The short period of the cardiac cycle makes visual inspection of the morphology over moderate to long time periods (i.e., >1 min) difficult. With arterial blood pressure, short segments (e.g., 30 s) and a combination of scalar metrics such as the beat duration, mean pressure, and the areas under the systolic and diastolic portions are used to attempt to quantify the useful characteristic of the morphology on a beat-by-beat basis [1]–[4]. Much of this research, called pulse contour analysis, has produced new methods of estimating clinically relevant parameters such as cardiac output, arterial compliance, and systemic vascular resistance [2], [5]–[10].

In most clinical settings, pressure signals are monitored continuously and at sufficiently high sampling rates to accurately capture the pulse morphology. Even so, no methodology exists that allows researchers to analyze how the morphology varies over moderate to long periods (>1 min) or to determine the relationship of pulse morphology to signal metrics such as the mean heart rate or pulse pressure.

We propose a new methodology, called the *morphologram*, that permits researchers to perform detailed visual analysis of the morphology of pressure signals. Conceptually, our methodology creates a family of estimates of the functional relationship between each point of the pulse morphology and a signal metric associated with each pulse. This methodology produces a 2-D image similar to a time-frequency analysis such as the spectrogram. Essentially, it presents a "top-down" view of the pulse morphology as it varies over time or in relation to a signal metric such as mean pressure, pulse pressure, or heart rate. We demonstrate the technique with examples of the pulse morphology variation in ICP signals acquired from pediatric patients with traumatic brain injuries.

A. Application in Intracranial Pressure

Traumatic brain injury (TBI) is a leading cause of death and disability in the United States [11]. Elevated ICP is common in TBI patients and can result in secondary injury due to cerebral ischemia [12]–[14]. Although there have been no randomized clinical trials, it is generally accepted that continuous monitoring of ICP signals has resulted in improved clinical outcome [12], [15], [16]. The mean ICP, usually defined as a 3–8 s moving average of the ICP signal, is the most common signal metric used to guide therapeutic interventions such as hyperventilation or mannitol administration, which tend to lower the mean ICP. Generally, clinicians intervene when the mean ICP is

Manuscript received February 3, 2006; revised January 3, 2007. This work was supported in part by the Thrasher Research Fund. *Asterisk indicates corresponding author*.

*T. Ellis is with the Biomedical Signal Processing Laboratory, Electrical and Computer Engineering Department, Portland State University, 1900 SW 4th Ave., Portland, OR 97201 USA (e-mail: taellis@pdx.edu; mcnames@pdx.edu).

J. McNames is with the Biomedical Signal Processing Laboratory, Electrical and Computer Engineering Department, Portland State University, Portland, OR 97201 USA (e-mail: taellis@pdx.edu; mcnames@pdx.edu).

M. Aboy is with the Electronics Engineering Technology Department, Oregon Institute of Technology, Portland, OR 97229 USA, the Biomedical Signal Processing Laboratory, Department of Electrical and Computer Engineering, Portland State University, Portland, OR 97201 USA, and also with the University of London, London WC1E 7HU, U.K. (e-mail: mateo@ieee.org).

Color versions of one or more of the figures in this paper are available online at http://ieeexplore.ieee.org.

Digital Object Identifier 10.1109/TBME.2007.892918

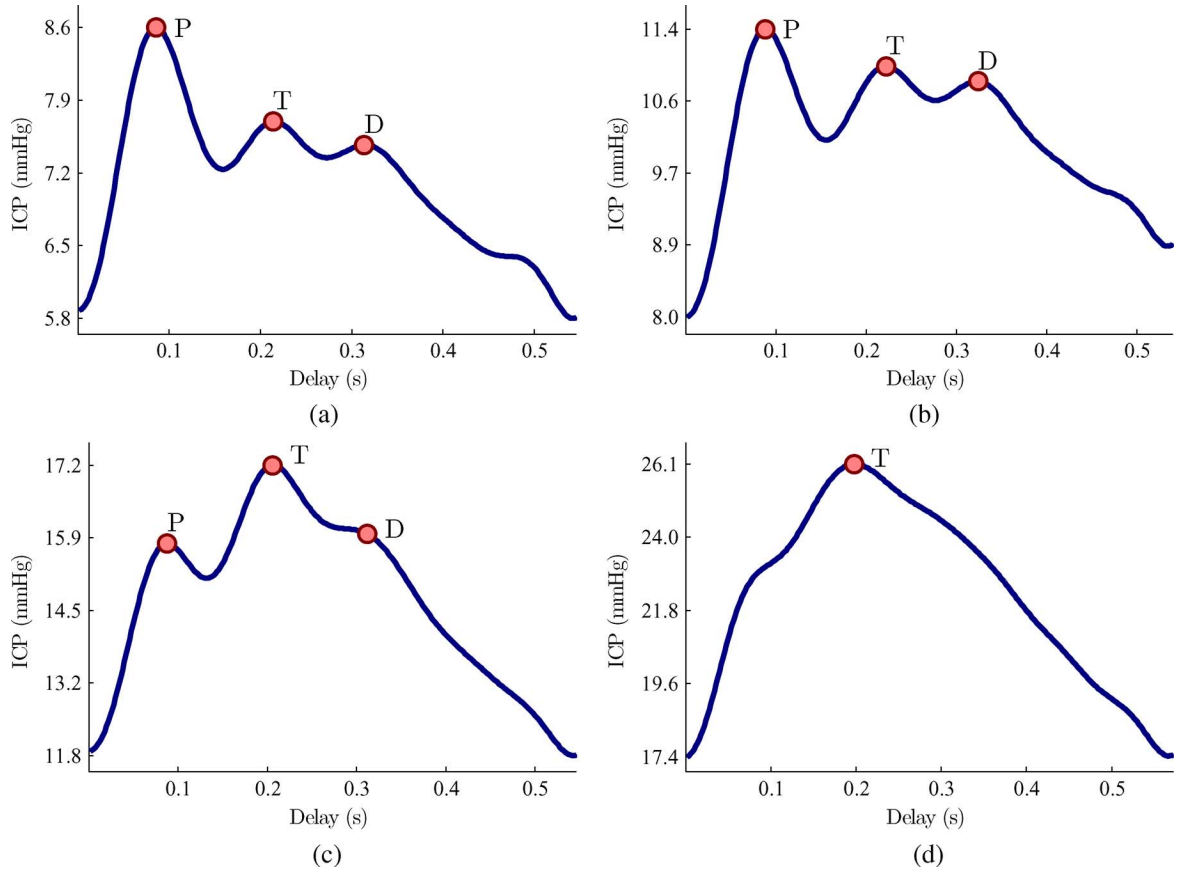

Fig. 1. Example of the ICP pulse morphology becoming more rounded, or sinusoidal, as the mean ICP increases. Peaks labeled are the percussion (P), tidal (T), and dichrotic (D). (a) $\mathrm{Mean\ ICP} = 7.12\ \mathrm{mmHg}$, (b) $\mathrm{Mean\ ICP} = 10.1\ \mathrm{mmHg}$, (c) $\mathrm{Mean\ ICP} = 14.7\ \mathrm{mmHg}$, and (d) $\mathrm{Mean\ ICP} = 22.5\ \mathrm{mmHg}$.

sustained above some threshold (usually 20 mmHg) [15], [16]. The optimal threshold for treatment undoubtedly varies across patients.

Other investigators have found that additional information about the clinical state of the patient, such as the cerebral compliance or integrity of cerebral autoregulation could be extracted from the ICP signal [15], [17], [18]. Several researchers have employed ICP pulse morphology to obtain additional information [15], [17]–[22]. Unlike most other cardiovascular pressure signals, the ICP pulse morphology typically contains three peaks, called the percussion, tidal, and dichrotic peaks, respectively (Fig. 1). The relative amplitudes of these peaks and depth of the valleys between them vary considerably across patients and, in many cases, in recordings from a single patient.

Morphologic changes have long been associated with changes in the mean ICP. In particular, as the mean ICP increases the pulse morphology frequently becomes more rounded, or sinusoidal (Fig. 1). Specifically, the tidal peak becomes dominant and makes the percussion and dichrotic peaks indiscernible. Since this often occurs with elevated mean ICP, the principal gauge of worsening patient condition, the rounding of the pulse morphology has been explained in the context of deteriorating mechanisms that control cerebral blood flow [13], [17], [22]–[25]. In a preliminary study we described a method for estimating the portion of the morphology that is independent of the mean ICP [26]. Examples demonstrated that in some cases the "residual morphology" contained significant patterns before and after therapeutic interventions, which suggests some variations in pulse morphology are not solely dependent on the mean ICP. This supports the hypothesis that the pulse morphology of ICP contains more information than can be explained by the mean ICP alone. The physiology and clinical importance of this transition to rounded morphology, however, varies over time and across patients, and remains an open area of research.

A number of ICP signal metrics have been proposed that indirectly estimate intracranial dynamics of interest [15], [17], [19], [20]. Most of these metrics are scalar parameters designed to quantify a single property of the ICP pulse morphology. These indices use methods such as spectral analysis [21], [22], [27] or pulse slope [22], [24]. Ideally, the additional information in the pulse morphology will help clinicians select a better course of therapy than is possible with the mean ICP alone. Developing methods to extract this information remains a significant research goal. To aid the development of these methods, analysis tools are needed that give a complete representation of the pulse morphology and how it varies with time or signal metrics of interest.

II. Methodology

Our method estimates the functional relationship between the pulse morphology and any scalar predictor variable (i.e., a signal

Fig. 2. Block diagram for the morphologram analysis algorithm.

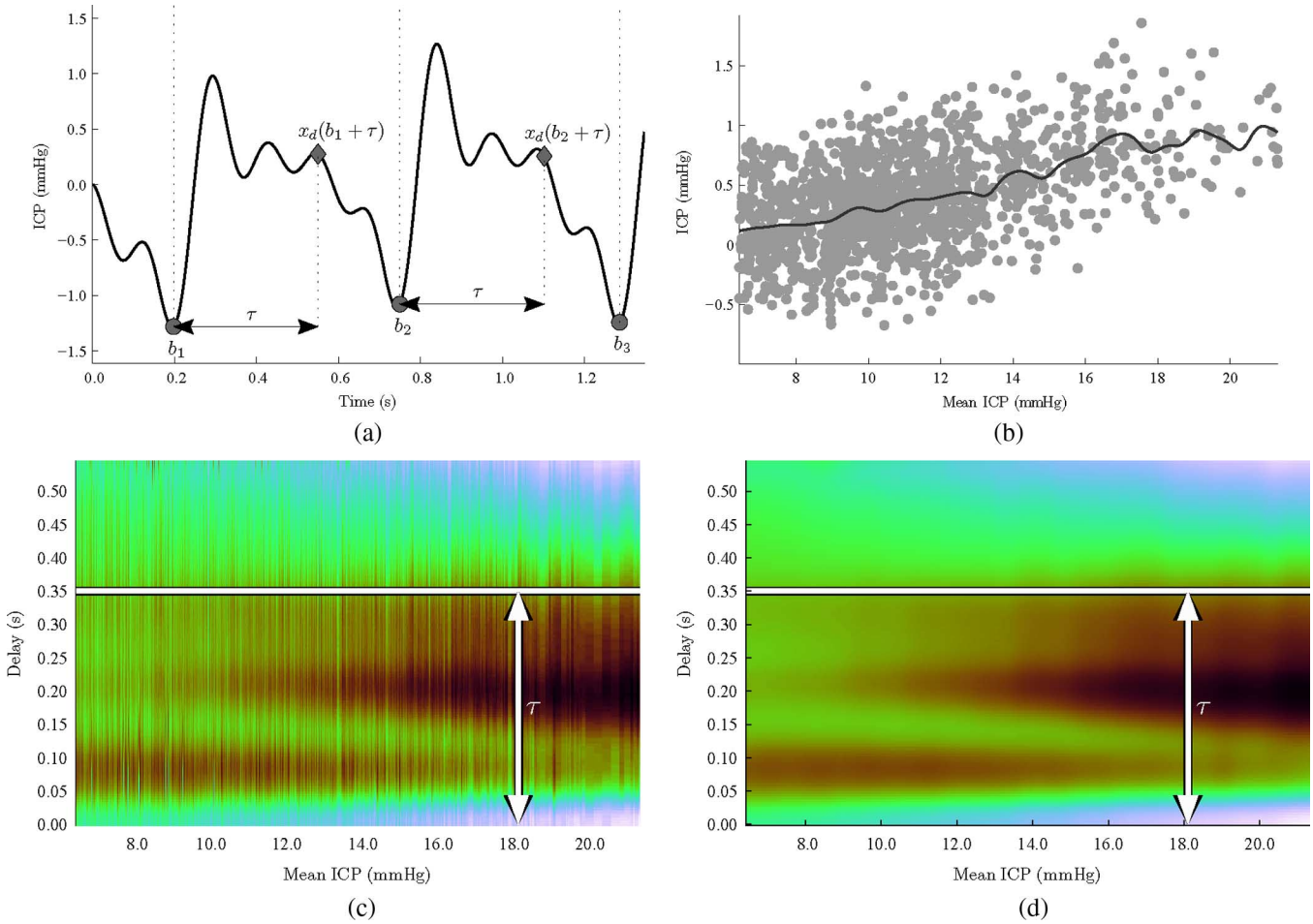

Fig. 3. (a) Segment of detrended ICP signal showing detected beat minima b_k and $x_d(b_k+\tau)$ at delay $\tau = 0.35$ s. (b) Corresponding scatter plot at delay $\tau = 0.35$ s showing the relative pressure of each pulse against its respective signal metric value (mean ICP in this case). Also shown is the smoothing fit. (c) Non-smoothed (nearest-neighbor interpolation) pseudo-color image showing expected morphology as a function of mean ICP. (d) Smoothed pseudo-color image showing expected morphology as a function of mean ICP. Smoothing in (b) corresponds to smoothing across the horizontal white line on the morphologram in (c) and (d). The total morphologram is constructed from this type of smoothing at each delay, τ.

metric) m by calculating $\hat{p}(\tau, m)$, an estimate of the expected pulse morphology given m at a delay τ seconds past the onset of the pulse. The method then creates a pseudo-color image of $\hat{p}(\tau, m)$ (i.e., the morphologram) that depicts the relationship of the estimated pulse morphology to m, similar in appearance to time-frequency analysis. The color scale used in the figures is described in [28]. In this section, we provide precise descriptions of each of the steps used to generate the morphologram. Fig. 2 shows a general block diagram of the morphologram analysis algorithm.

A. Event Detection and Pulse Fiducial Points

The morphologram requires the detection of the onset of each pulse. Any fiducial point could suffice, but in pressure signals the diastolic minima preceding each pulse (i.e., the "beat" minima) is convenient because it can be detected easily and represents the onset of pressure following each cardiac contraction. The times of these events are denoted as b_k, as shown in the application to an ICP signal [Fig. 3(a)]. We represent the ordered set of these beat indices as $\mathcal{B} = \{b_1, b_2, \ldots, b_{N_b}\}$, where N_b is the number of beats in the observed signal segment. Current software programs permit precise and consistent detection of heart beats even in the presence of arrhythmias or damped pressure waveforms [29]. For the off-line examples in this paper we detected the fiducial points with an automatic beat detection algorithm [30].

B. Signal Metric Association

Obtaining estimates of the pulse morphology given a signal metric requires associating each pulse with a signal metric, denoted m_k. We describe here how we associate a mean pressure with each beat. In research applications and the clinical setting the mean pressure is usually defined to be a moving window

average of 3–8 s. The purpose of this is to eliminate high frequency fluctuations in the signal due to respiration and the pulsatile component synchronous with the cardiac cycle. We used a zero-phase, noncausal elliptic IIR lowpass filter with a cutoff frequency of 0.3 Hz

$$\bar{x}(t) = x(t) * h_{\mathrm{LP}}(t) \tag{1}$$

where $x(t)$ is the pressure signal, $h_{\mathrm{LP}}(t)$ is the impulse response of the lowpass filter, and $*$ denotes convolution. This filter produces an estimate of the mean that is similar to a moving average estimate, but has better attenuation of the respiratory and cardiac components. Since this is a noncausal filter, this method is only applicable for off-line analysis. The mean pressure associated with each pulse, m_k, is then computed as the mean pressure at the midpoint between beat minima, $m_k = \bar{x}(t_k)$ where $t_k = (b_k + b_{k+1})/2$.

C. Removal of Low Frequency Content

The pulse morphology of interest is represented by the repeated fluctuations in the pressure signal that occur with contractions of the heart. This signal is nearly periodic with a fundamental frequency equal to the heart rate, so the power spectral density of the pulse morphology occurs at frequencies at or above the heart rate. Other low-frequency content is also present in $x(t)$ due to baseline drift, respiratory fluctuations, and other effects, such as A, B, and C waves in ICP signals [31]. We isolate the pulse morphology of interest from these low-frequency components with a highpass filter

$$x_{\mathrm{D}}(t) = x(t) * h_{\mathrm{HP}}(t) \tag{2}$$

where $h_{\mathrm{HP}}(t)$ is the impulse response of the highpass filter. We used a zero-phase, noncausal elliptic IIR highpass filter with a cutoff frequency of 0.3 Hz. Thus, the morphology of the kth observed pulse is $x_{\mathrm{D}}(b_k + \tau)$.

D. Pulse Morphology Estimation

The method creates a functional relationship between the pulse morphology and the signal metric by estimating the expected pulse morphology given the signal metric. We create a family of estimates for fixed values of τ ranging from 0 to the duration of the pulse morphology. For pressure signals, the pulse morphology duration is defined as the average inter-beat interval. We model the relationship between the observed morphologies and the signal metric as

$$x_{\mathrm{D}}(b_k + \tau) = p(\tau, m_k) + \varepsilon_k \tag{3}$$

where

$$p(\tau, m_k) = \mathrm{E}\left[x_{\mathrm{D}}(b_k + \tau) | m_k\right] \tag{4}$$

is the expected morphology given the observed signal metric, and ε_k is an independent, zero-mean random variable that models the variation in $x_{\mathrm{D}}(b_k + \tau)$ that cannot be explained by m_k. Our goal is to calculate and display $\hat{p}(\tau, m)$, an estimate of the expected pulse morphology given m.

Fig. 3(c) shows the un-smoothed pulse morphology $x_{\mathrm{D}}(b_k + \tau)$ of an ICP signal over all of the observed mean pressure values. The true relationship between the expected morphology and the signal metric can be more accurately estimated by applying a nonparametric regression smoother to estimate $p(\tau, m)$ for fixed lags. Smoothing decreases the variance of the estimate and more accurately depicts the relationship of the pulse morphology to the signal metric. Fig. 3(d) shows the estimated pulse morphology after smoothing with respect to the signal metric. Fig. 3(b) shows the smoothing fit across all observed mean pressure values at a fixed lag $\tau = 0.35$ s.

Any nonparametric method of regression smoothing could be applied. For the examples in this paper we used a kernel smoother

$$\hat{p}(\tau, m) = \frac{\sum_{k=1}^{N_b} x_{\mathrm{D}}(b_k + \tau) f_\sigma\left(|m - m_k|\right)}{\sum_{k=1}^{N_b} f_\sigma\left(|m - m_k|\right)} \tag{5}$$

where $f(\cdot)$ is a unimodal symmetric density function and σ controls the kernel width. We used a truncated Gaussian kernel function

$$f_\sigma(u) = \begin{cases} \frac{1}{\sigma} \mathrm{e}^{-\frac{u^2}{2\sigma^2}}, & |u| \le 5 \\ 0, & |u| > 5 \end{cases} \tag{6}$$

where σ is 2% of the observed range of m_k

$$\sigma = 0.02 \left[\max_k(m_k) - \min_k(m_k)\right]. \tag{7}$$

III. Results and Discussion

We demonstrate the morphologram on ICP signals acquired from the Pediatric Intensive Care Unit (PICU) at Doernbecher Children's Hospital, Oregon Health and Science University. First we give an example with several additional plots that show the performance of the morphologram. Next, we show six examples of the morphologram applied to ICP signals and discuss some of the insights that can be gained from this type of analysis.

A. Supplementary Plots

Fig. 4 shows an example of the morphologram applied to an ICP signal along with six supplementary plots that can help the end-user analyze the pulse morphology more thoroughly. The primary plot is the morphologram [Fig. 4(A)], which shows the pulse morphology as it varies over mean pressure. This is similar in appearance to time-frequency analysis, except with the signal metric on the horizontal axis and delay past pulse onset on the vertical axis. Fig. 4(B) shows the color scale used to encode the pulse morphology in the morphologram. In this example, at low mean ICP the first dark band represents the percussion peak and the second represents the tidal peak; the dichrotic peak also appears, though very faintly. The morphologram reveals that the tidal peak increases in amplitude and merges with the percussion peak starting at about $m = 12$ mmHg, forming a large and very dark band at high mean ICP (the "rounded" morphology).

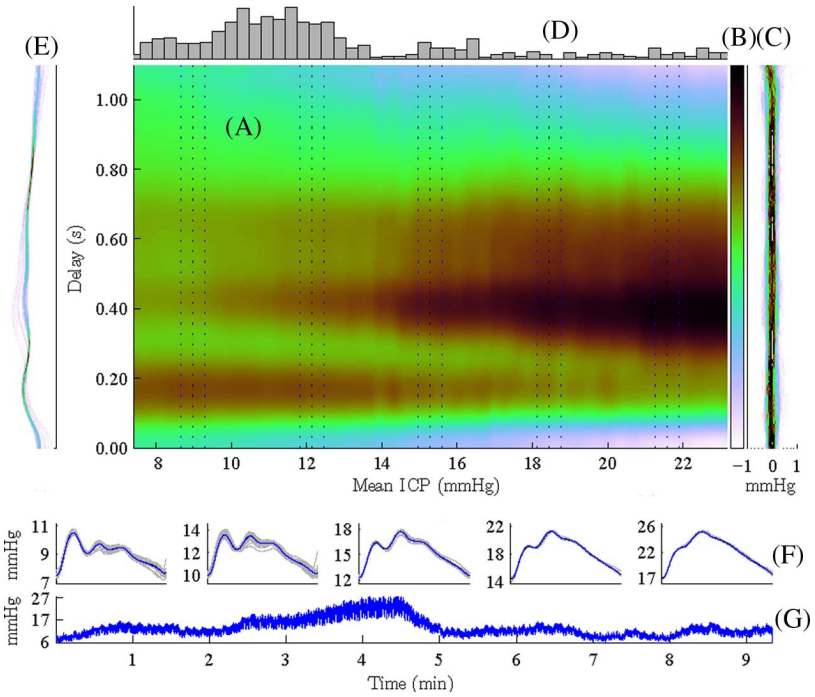

Fig. 4. ICP morphologram with (A) signal metric $m = \text{mean ICP}$. Supplementary plots include (B) pseudo-color scale, (C) pseudo-colored residual histogram, (D) signal metric histogram, (E) pseudo-colored morphology histogram, (F) pulse morphology overlap plots, and (G) original signal and mean .

Fig. 4C, shows a 2-D histogram of the estimation residuals at each delay, $x_{\mathrm{D}}(b_k + \tau) - \hat{p}(\tau, m_k)$. Its vertical axis corresponds to the vertical axis (τ) of the morphologram. The color scale uses a continuous range from light pink (smallest non-zero density) to dark red (largest density). This histogram is useful for identifying the delays at which the observed morphology $x_{\mathrm{D}}(b_k + \tau)$ differs the most from the expected morphology $\hat{p}(\tau, m_k)$.

Fig. 4(D) shows a histogram of the observed signal metrics m. This is helpful for identifying regions of sparse data. In these regions the estimated morphology $\hat{p}(\tau, m)$ will be less accurate.

Fig. 4(E) shows a 2-D histogram of the observed morphologies $x_{\mathrm{D}}(b_k + \tau)$. This uses the same color scale as Fig. 4(C) and has the same vertical axis (τ) as the morphologram. This is useful for identifying the dominant observed morphology and the variability of the morphology.

Fig. 4(F) shows five overlap plots of the observed pulse morphologies (light gray) over the same five segments of m and the estimated morphology at the center of the range (dark blue). This is useful for investigating examining the morphology with better resolution in several distinct regions of the morphologram.

Fig. 4(G) shows the original signal and trend in the time domain

B. Examples

We applied the morphologram to two ICP signals obtained from pediatric patients with TBI admitted to the Intensive Care Unit at the Doernbecher Children's Hospital. The data acquisition protocol was reviewed and approved by the Institutional Review Board at Oregon Health and Science University, and the requirement on informed consent was waived. The ICP signals were interpolated using a polyphase filter implementation from an original sample rate of $f_s = 125$ Hz to 250 Hz to increase the resolution of the morphologram. The additional examples used four signal metrics (m): mean ICP [Fig. 5(c) and (d)], time [Fig. 5(a) and (b)], ICP pulse pressure [Fig. 5(e)], and mean arterial pressure (MAP) [Fig. 5(f)]. We obtained the MAP in the same manner as that used to obtain the mean ICP (Section II-B). The ICP pulse pressure is defined as the systolic ICP minus the diastolic ICP [17], [32]. We calculated the pulse pressure on a beat-by-beat basis, in which the pulse pressure of the kth beat is

$$x_{\mathrm{pp}}(b_k) = \max_{\tau}\left[x(b_k + \tau)\right] - x(b_k) \tag{8}$$

as in [33]. This maximum was constrained for values of $\tau > 0$ and less than the average inter-beat interval.

1) ICP Pulse Morphology Versus Time: Fig. 5(a) and (b) uses the morphologram to display how the ICP pulse morphology varies over time. In Fig. 5(a), both the percussion and tidal peaks appear as dark bands for the first 30 min. This suggests they had a similar amplitude over that time, and the two left-most pulse overlays confirm this. The dichrotic peak also appears faintly during this time interval. Between about 35 and 50 min, a wide dark band appears, indicating the emergence of a dominant tidal peak. This happens during the period of acute hypertensive ICP, as shown in the time domain signal. After the signal returns to pre-hypertensive levels (at about 50 min), however, the pulse morphology does not return to its pre-hypertensive state. This may suggest a deterioration in brain compliance that would be undetectable without the morphologram.

In contrast, the time morphologram applied to the second signal [Fig. 5(b)] tells a different story. Here only one peak appears, though as shown during the period of mild hypertension,

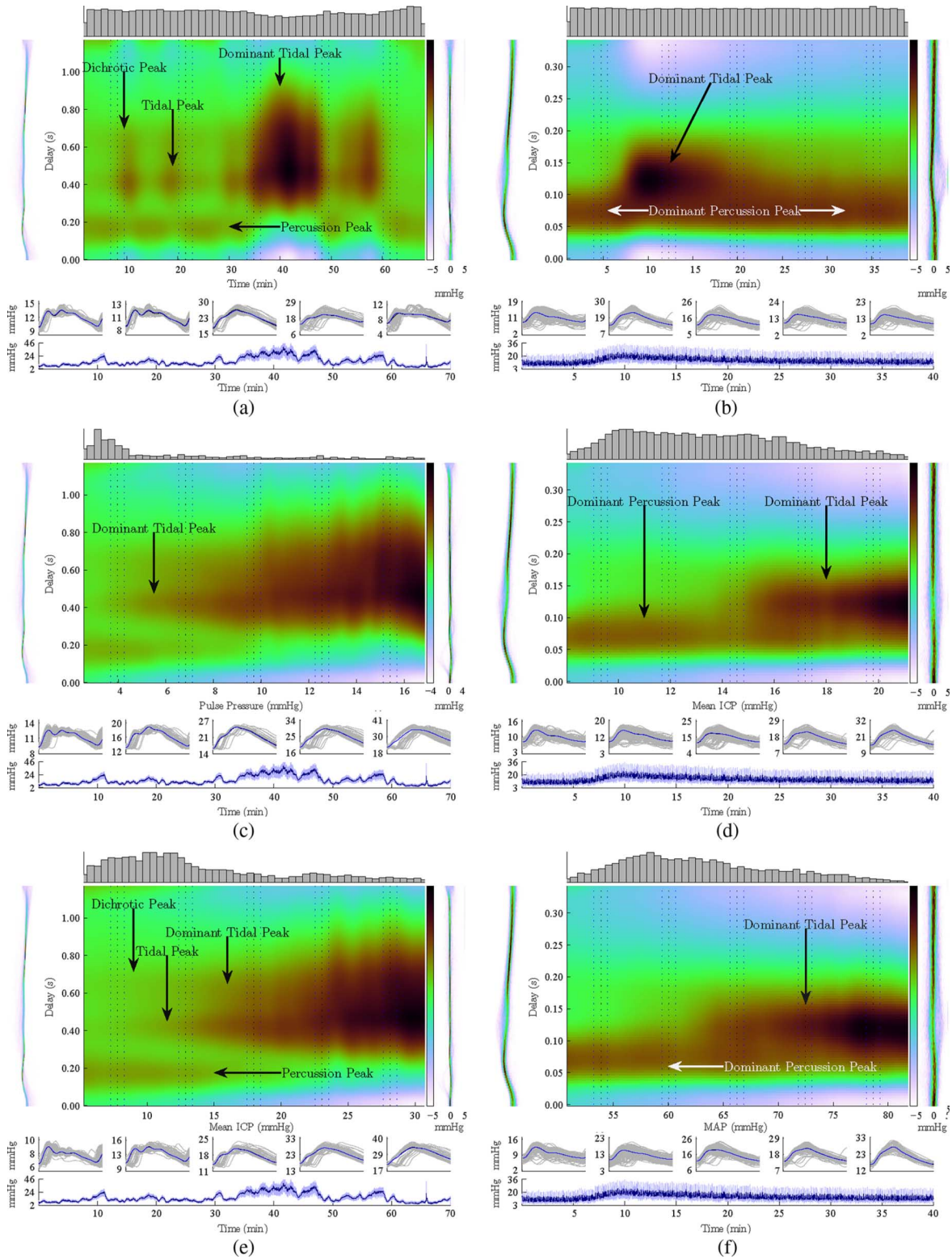

Fig. 5. Examples of the morphologram applied to two ICP signals with four different signal metrics m. (a) Signal 1 $m = \mathrm{Time}$, (b) Signal 2 $m = \mathrm{Time}$, (c) Signal 1 $m = \mathrm{mean\ ICP}$, (d) Signal 2 $m = \mathrm{mean\ ICP}$, (e) Signal 1 $m = \mathrm{Pulse-Pressure}$, and (f) Signal 2 $m = \mathrm{MAP}$.

the dominant feature switches from a narrow percussion peak to a wide tidal peak of higher amplitude.

2) Variation With Mean ICP: Figs. 4 and 5(c) and (d), show the morphologram with the mean ICP as the signal metric. In Figs. 4 and 5(c), the morphologram clearly shows two distinct peaks (percussion and tidal) at low mean ICP, and the dichrotic peak is faintly visible. As mean ICP increases, the tidal peak becomes dominant and the morphology appears to have a single peak with high amplitude and long duration. This is the "rounding" phenomenon, shown as the wide dark band.

Fig. 5(d), in contrast, shows less distinct percussion and tidal peaks with a subtler transition from a dominant percussion peak at low mean ICP to a dominant tidal peak at high mean ICP.

3) ICP Pulse Morphology Versus Pulse Pressure: Fig. 5(e) shows the ICP pulse morphology versus pulse pressure. The relationship expressed in Fig. 5(e) is quite similar to that in Fig. 5(c), with the tidal peak becoming dominant at about 5 mmHg. This is consistent with the expected correlation between mean ICP and pulse pressure. More importantly, it suggests the pulse pressure may provide no more information about the ICP morphology than is available from the mean ICP. This is significant because the pulse pressure is more difficult to calculate and is not readily available through most commercial ICP monitors.

4) ICP Pulse Morphology Versus Mean ABP: Fig. 5(f) shows the relationship between the ICP pulse morphology and MAP. The morphologram is similar to Fig. 5(d), suggesting that for this signal, the relationship of pulse morphology with MAP is similar to the relationship with mean ICP. Many studies have explored the relationship between MAP and mean ICP [15], [34], [35] but we are not aware of any studies that have examined the relationship of MAP to ICP pulse morphology.

IV. Conclusion

The morphologram is a signal analysis tool that displays an estimate of the pulse morphology. The pulse morphology is known to contain potentially useful clinical information but is difficult to study in the time domain without the aid of a tool such as the morphologram. The morphologram can estimate the relationship between the pulse morphology and time, or *any* signal metric.

The morphologram is an off-line analysis tool that relies on established signal processing techniques, nonparametric regression, and an automatic beat detection algorithm. Although the morphologram is best suited to exploratory analysis to aid in the development of signal metrics, it could also be easily be adapted for real-time monitoring of pulse morphology in a clinical setting.

The morphologram could also be applied to other types of signals that can be modeled as a point process consisting of a series of events that generate a consistent morphology. For example, this same methodology could be applied to extracellular neuronal recordings, respiratory waveforms, and electrocardiograms.

References

[1] K. Wesseling, R. Purschke, N. Smith, H. Wüst, B. de Wit, and H. Weber, "A computer module for the continuous monitoring of cardiac output in the operating theatre and the ICU," *Acta Anaesthesiol Belg*, vol. 27, pp. 327–341, 1976, suppl.

[2] G. McVeigh, C. Bratteli, D. Morgan, C. Alinder, S. Glasser, S. Finkelstein, and J. Cohn, "Age-related abnormalities in arterial compliance identified by pressure pulse contour analysis: Aging and arterial compliance," *Hypertension*, vol. 33, no. 6, pp. 1392–1398, Jun. 1999.

[3] O. Göodje, C. Thiel, P. Lamm, H. Reichenspurner, C. Schmitz, A. Schütz, and B. Reichart, "Less invasive, continuous hemodynamic monitoring during minimally invasive coronary surgery," *Ann. Thorac Surg.*, vol. 68, no. 4, pp. 1532–1536, Oct. 1999.

[4] N. Linton and R. Linton, "Estimation of changes in cardiac output from the arterial blood pressure waveform in the upper limb," *Br. J. Anaesth.*, vol. 86, no. 4, pp. 486–496, Apr. 2001.

[5] J. C. Chaney and S. Derdak, "Minimally invasive hemodynamic monitoring for the intensivist: Current and emerging technology," *Crit. Care Med.* vol. 30, no. 10, pp. 2338–2345, Oct. 2002 [Online]. Available: http://www.dx.doi.org/10.1097/01.CCM.000002918657736.02

[6] G. E. McVeigh, P. K. Hamilton, and D. R. Morgan, "Evaluation of mechanical arterial properties: Clinical, experimental and therapeutic aspects," *Clin. Sci. (Lond)*, vol. 102, no. 1, pp. 51–67, Jan. 2002.

[7] O. Gödje, K. Höke, A. E. Goetz, T. W. Felbinger, D. A. Reuter, B. Reichart, R. Friedl, A. Hannekum, and U. J. Pfeiffer, "Reliability of a new algorithm for continuous cardiac output determination by pulse-contour analysis during hemodynamic instability," *Crit. Care Med.*, vol. 30, no. 1, pp. 52–58, Jan. 2002.

[8] G. Rödig, C. Prasser, C. Keyl, A. Liebold, and J. Hobbhahn, "Continuous cardiac output measurement: Pulse contour analysis vs thermodilution technique in cardiac surgical patients," *Br. J. Anaesth.*, vol. 82, no. 4, pp. 525–530, Apr. 1999.

[9] L. Resnick, D. Militianu, A. Cunnings, J. Pipe, J. Evelhoch, R. Soulen, and M. Lester, "Pulse waveform analysis of arterial compliance: Relation to other techniques, age, and metabolic variables," *Am. J. Hypertens.*, vol. 13, no. 12, pp. 1243–1249, Dec. 2000.

[10] J. Cohn, S. Finkelstein, G. McVeigh, D. Morgan, L. LeMay, J. Robinson, and J. Mock, "Noninvasive pulse wave analysis for the early detection of vascular disease," *Hypertension*, vol. 26, no. 3, pp. 503–508, Sep. 1995.

[11] P. Adelson and P. Kochanek, "Head injury in children," *J. Child Neurol.*, vol. 13, no. 1, pp. 2–15, 1998.

[12] P. Adelson, S. Bratton, N. Carney, R. Chesnut, H. du Cordray, B. Goldstein, P. Kochanek, H. Miller, M. Partington, N. Selden, C. Warden, and D. Wight, "Guidelines for the acute medical management of traumatic brain injury in infants, children, and adolescents," *Crit. Care Med.*, vol. 31, no. 6 (Suppl), pp. S417–S490, Jun. 2003.

[13] B. North, "Intracranial pressure monitoring," in *Head Injury*, P. Reilly and R. Bullock, Eds. London, U.K.: Chapman & Hall, 1997, pp. 209–216.

[14] J. F. Kraus, A. Rock, and P. Hemyari, "Brain injuries among infants, children, adolescents, and young adults," *Am. J. Diseases Children*, vol. 144, no. 6, pp. 684–691, Jun. 1990.

[15] M. Czosnyka and J. D. Pickard, "Monitoring and interpretation of intracranial pressure," *J. Neurol. Neurosurg. Psychiatry*, vol. 75, no. 5, pp. 813–821, Jun. 2004.

[16] T. G. Luerssen, "Intracranial pressure: Current status in monitoring and management," *Sem. Pediatr. Neurol.*, vol. 4, no. 3, pp. 146–155, Sep. 1997.

[17] C. Contant, C. Robertson, J. Crouch, S. Gopinath, R. Narayan, and R. Grossman, "Intracranial pressure waveform indices in transient and refractory intracranial hypertension," *J. Neurosci. Meth.*, vol. 57, no. 1, pp. 15–25, Mar. 1995.

[18] H. D. Portnoy, M. Chopp, C. Branch, and M. B. Shannon, "Cerebrospinal fluid pulse waveform as an indicator of cerebral autoregulation," *J. Neurosurg.*, vol. 56, no. 5, pp. 666–678, May 1982.

[19] M. Balestreri, M. Czosnyka, L. Steiner, E. Schmidt, P. Smielewski, B. Matta, and J. Pickard, "Intracranial hypertension: What additional information can be derived from ICP waveform after head injury?," *Acta Neurochir (Wien)*, vol. 146, no. 2, pp. 131–141, Feb. 2004.

[20] M. Czosnyka, E. Guazzo, M. Whitehouse, P. Smielewski, Z. Czosnyka, P. Kirkpatrick, S. Piechnik, and J. Pickard, "Significance of intracranial pressure waveform analysis after head injury," *Acta Neurochirurgica*, vol. 138, no. 5, pp. 531–541, 1996.

[21] M. J. Dubin, G. Magram, and A. K. Prasad, "Intracranial pressure waveform analysis: Computation of pressure transmission and waveform shape indicators," *Neurological Res.*, vol. 20, no. 6, pp. 533–541, Sep. 1998.

[22] M. Chopp and H. Portnoy, "Systems analysis of intracranial pressure. Comparison with volume-pressure test and CSF-pulse amplitude analysis," *J. Neurosurg.*, vol. 53, no. 4, pp. 516–527, Oct. 1980.

[23] H. D. Portnoy and M. Chopp, "Cerebrospinal fluid pulse wave form analysis during hypercapnia and hypoxia," *Neurosurgery*, vol. 9, no. 1, pp. 14–27, 1981.

[24] E. L. Foltz, J. P. Blanks, and K. Yonemura, "CSF pulsatility in hydrocephalus: Respiratory effect on pulse wave slope as an indicator of intracranial compliance," *Neurological Res.*, vol. 12, no. 2, pp. 67–74, Jun. 1990.

[25] D. Doyle and P. Mark, "Analysis of intracranial pressure," *J. Clin. Monit.*, vol. 8, no. 1, pp. 81–90, Jan. 1992.

[26] T. Ellis, J. McNames, and B. Goldstein, "Residual pulse morphology visualization and analysis in pressure signal," in *Proc. 27th Annu. Int. Conf. IEEE Engineering in Medicine and Biology*, Shanghai, China, Sep. 1–4, 2005, pp. 2880–2883.
[27] I. R. Piper, J. D. Miller, N. M. Dearden, J. R. S. Leggate, and I. Robertson, "Systems analysis of cerebrovascular pressure transmission: An observational study in head-injured patients," *J. Neurosurg.*, vol. 73, no. 6, pp. 871–880, Dec. 1990.
[28] J. McNames, "An effective color scale for simultaneous color and gray-scale publications," *IEEE Signal Process. Mag.*, vol. 23, no. 1, pp. 82–87, Jan. 2006.
[29] J. van Lieshout and K. Wesseling, "Continuous cardiac output by pulse contour analysis?," *Br. J. Anaesth.*, vol. 86, no. 4, pp. 467–469, Apr. 2001.
[30] M. Aboy, J. R. Fernández, and R. C. Hermida, "Methodological considerations in the evaluation of the duration of action of antihypertensive therapy using ambulatory blood pressure monitoring," *Blood Press Monit.*, vol. 10, no. 3, pp. 111–115, Jun. 2005.
[31] N. Lundberg, "Continuous recording and control of ventricular fluid pressure in neurosurgical practice," *Acta Psychiatrica et Neurologica Scandinavica*, vol. 36, no. Suppl. 149, pp. 1–193, 1960.
[32] C. Avezaat, J. van Eijndhoven, and D. Wyper, "Cerebrospinal fluid pulse pressure and intracranial volume-pressure relationships," *J. Neurol. Neurosurg. Psychiatry*, vol. 42, no. 8, pp. 687–700, Aug. 1979.
[33] M. Aboy, J. McNames, T. Thong, C. R. Phillips, M. S. Ellenby, and B. Goldstein, "A novel algorithm to estimate the pulse pressure variation index," *IEEE Trans. Biomed. Eng.*, vol. 51, no. 12, pp. 2198–2203, Dec. 2004.
[34] M. Balesteri, M. Czosnyka, L. Steiner, E. Schmidt, B. Smielewski, B. Matta, and J. Pickard, "Intracranial hypertension: What additional information can be derived from ICP waveform after injury?," *Acta Neurochirurgica*, vol. 146, no. 2, pp. 131–141, Feb. 2004.
[35] R. Panerai, "Assessment of cerebral pressure autoregulation in humans-a review of measurement methods," *Physiol. Meas.*, vol. 19, no. 3, pp. 305–338, Aug. 1998.

Tim Ellis (S'04) received the B.S. degree in electrical engineering from Portland State University, Portland, OR, in 2006, where he is currently working toward the M.S. degree.

He has been a member of the Biomedical Signal Processing Laboratory (BSP), Portland State University, since 2004. His research focus has been extracting information from physiologic signals of pediatric traumatic brain injury patients. His other interests include signal processing, estimation theory, and engineering education.

James McNames (M'99–SM'03) received the B.S. degree in electrical engineering from California Polytechnic State University, San Luis Obispo, in 1992, and the M.S. and Ph.D. degrees in electrical engineering from Stanford University, Stanford, CA, in 1995 and 1999, respectively.

He has been with the Electrical and Computer Engineering Department at Portland State University, Portland, OR, since 1999, where he is currently an Associate Professor. In fall 2000, he founded the Biomedical Signal Processing (BSP) Laboratory at Portland State University, where he is currently the Director. The mission of the BSP Laboratory is to advance the art and science of extracting clinically significant information from physiologic signals. Members of the BSP Laboratory primarily focus on clinical projects in which the extracted information can help physicians or medical devices make better critical decisions and improve patient outcome. He has published over 100 peer reviewed journal and conference papers. His primary research interest is statistical signal processing with applications to biomedical engineering.

Mateo Aboy (M'98) was born in Pontevedra, Spain, in 1980. He received the dual B.S. degree in both electrical engineering and physics (with a minor in mathematics) and the M.S. degree in electrical and computer engineering from Portland State University, Portland, OR, in 2002 and 2004, respectively, and the M.Phil. (DEA) degree in telecommunications engineering and the Ph.D. degree in electrical engineering from the University of Vigo (ETSIT), Spain, in 2004 and 2005, respectively. He is currently working toward the MBA degree in international business and management at the University of London, London, U.K.

He joined the faculty of the Oregon Institute of Technology (OIT-Portland), Portland, OR, during the 2004/2005 academic year as a tenure-track Assistant Professor and has been a research member of the Biomedical Signal Processing Laboratory at PSU since September 2000. He is currently the Program Director of the Electronics Program at OIT-Portland. His research is primarily focused on statistical signal processing and its applications to solve biomedical engineering problems. He has published over 50 scholarly articles and proceedings, including nine journal papers in the IEEE TRANSACTIONS ON BIOMEDICAL ENGINEERING.

Dr. Aboy is a full member of the Scientific Research Society (Sigma XI), a lifetime honorary member of the Golden Key Honor Society, a past Chapter President of the International Electrical Engineering Honor Society (HKN), and a past Corresponding Secretary of the National Engineering Honor Society (TBP). He currently serves as the President of the Oregon Chapter of the IEEE Education Society and as an Associate Editor for the *IEEE Revista Iberoamericana de Tecnologías del Aprendizaje Journal* (IEEE-RITA).